Cross sections for neutral-current neutrino scattering on ^{208}Pb

N. Jachowicz,* K. Heyde,† and J. Ryckebusch
Institute for Subatomic and Radiation Physics, Ghent University, Proeftuinstraat 86, B-9000 Gent, Belgium
(Received 5 March 2002; published 1 November 2002)

We present continuum random phase approximation (CRPA) calculations for neutral-current neutrino scattering off ^{208}Pb. These reactions are of interest for the terrestrial detection of supernova neutrinos. We fold the computed cross sections with a Fermi-Dirac distribution to obtain information about these processes and examine the dependence of the response on the spectrum parameters. The experimental interest in neutron knockout induced by neutrino interactions on ^{208}Pb motivated an analysis of the CRPA branching ratios and single-particle knockout channels. We investigate the role of the single-particle wave functions and the residual interaction for the response. We compare our cross sections with previous work.

DOI: 10.1103/PhysRevC.66.055501 PACS number(s): 13.15.+g, 25.30.−c, 24.10.−i

I. INTRODUCTION

As the field of neutrino physics is becoming ever more exciting, growing attention is being paid to the use of neutrinos as a potential source of information about other physical processes. One of the most important events where neutrinos play a prominent role is the end of the life of a massive star in a type-II supernova explosion. Most of the energy released in the gravitational collapse and the cooling of the protoneutron star is carried away by neutrinos of all flavors. Interacting only by means of the weak interaction, these neutrinos can escape from deep into the center of the star. Therefore neutrinos are exquisite tools to probe the inner core of the star, looking far beyond the reach of the more easily detected photons. Detecting the neutrinos witnessing the processes going on in the center of the star and studying their energy, time, and flavor distributions would therefore provide precious information about the processes driving the supernova explosion, the fate of the star, and about neutrino properties as mass and oscillation characteristics [1,2].

The advent of neutrino observatories and the neutrino signal of SN1987*A* further enhanced this interest in supernova-neutrino detection. Proposed experiments as OMNIS and LAND [3,4] plan to detect the neutrino signal from a future galactic supernova. The Z dependence of the neutrino-nucleus cross section favors the interaction of neutrinos with massive nuclei. Hence, ^{208}Pb seems a well-suited target and has indeed been proposed as a possible detection material in these projects. In addition, ^{208}Pb is frequently used as a shielding material in experiments that probe neutrinos. For all the above reasons it is of the utmost importance to have reliable cross-section calculations available for neutrino scattering on this nucleus.

As a closed-shell nucleus, ^{208}Pb is well suited for theoretical studies. Previous studies of neutrino scattering on ^{208}Pb include the random-phase approximation (RPA) calculation of Refs. [5,6] and the work of Ref. [7], an approach combining empirical data with a Goldhaber-Teller treatment for the evaluation of forbidden transitions. Important discrepancies, however, exist between these approaches, necessitating a further study of these reactions. Therefore we extended the applications of our continuum RPA (CRPA) formalism [8] to the study of cross sections for neutral-current neutrino scattering on ^{208}Pb. The proposed experiments plan to detect the neutrinos indirectly, through the neutron knockout they induce. Therefore, the fact that the CRPA calculation does not include transitions to bound states does not restrict the validity of our results.

Previous studies [5,7] point to the fact that charged-current cross sections are substantially larger than cross sections for neutral-current scattering. Despite this, the latter will provide important information. The reason for this is twofold. First, the energy of supernova neutrinos is too small to produce a massive μ or τ lepton, limiting the number of neutrinos that will participate in charged-current scattering. Moreover, charged-current antineutrino scattering is suppressed due to Pauli blocking. Thus, only electron-neutrino charged-current reactions will be important while all neutrino and antineutrino flavors take part in neutral-current scattering off ^{208}Pb in a terrestrial detector. The main strength of the proposed detector is due to the fact that through neutral-current interactions heavy flavor neutrinos can be detected too, while most other detectors would observe a supernova through the electron-neutrino and -antineutrino emission. The plan to use the OMNIS detector as a flavor filter and to examine the oscillation characteristics of the arriving supernova neutrinos makes the study of the neutral-current contribution indispensable for a complete picture of the phenomena of interest.

II. FORMALISM

The $^{208}\mathrm{Pb}(\nu,\nu')^{208}\mathrm{Pb}^*$ results presented here are obtained within a CRPA formalism based on a Green's-function approach [8–10]. It iterates the lowest-order term of the two-body polarization propagator to all orders. In this way particle-hole (p-h) configurations out of the correlated ground state are taken into account, but there is no coupling to $2p$-$2h$, $3p$-$3h$, ... states. The major advantage of our approach is that the continuum part of the single-particle energy spectrum can be treated exactly. In many other frameworks, a discretization and/or cutoff procedure is applied to

*Email address: natalie.jachowicz@rug.ac.be
†Present address: EP-ISOLDE, CERN, Geneva, Switzerland.

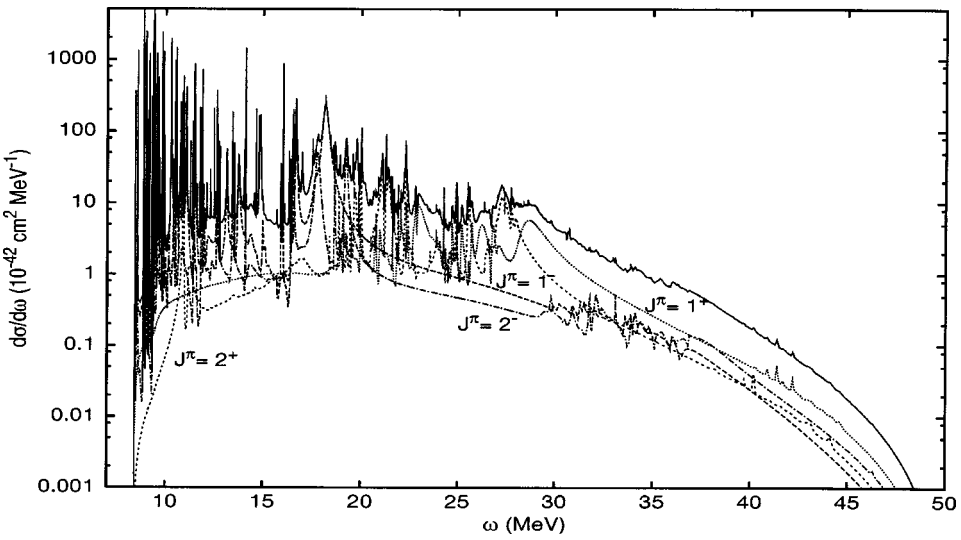

FIG. 1. Dominant multipole contributions to the differential ^{208}Pb(ν, ν')^{208}Pb* cross section: $J^\pi=1^+$ (dotted line), $J^\pi=1^-$ (dashed), $J^\pi=2^+$ (short dashed), and $J^\pi=1^+$ (dash dotted). The cross section was obtained using a self-consistent Hartree-Fock Skyrme CRPA calculation. The full line gives the total cross section with all multipoles up to $J=6$ included, the incoming neutrino energy is 50 MeV.

the energy continuum. In an attempt to estimate the model uncertainties in our calculations, we have performed the CRPA calculations with two different sets of single-particle wave functions and energies. First, we used the set of proton and neutron wave functions obtained through a Hartree-Fock calculation, and second, a Woods-Saxon potential was used to generate the single-particle wave functions [11]. We have used both of these sets in combination with two different choices for the residual interaction; a Skyrme force variant SkE2 [12,13] and a standard Landau-Migdal force [14]. The SkE2 Skyrme parametrization was designed to reproduce ground-state as well as excited-state properties for nuclei over the whole mass table. These extended Skyrme parametrizations were shown to reproduce well the excitation energies and multipole strength distribution in ^{208}Pb [13]. Moreover, the CRPA formalism has been successfully applied to the study of electron-induced and photoinduced nucleon knockout from nuclei [15], for inclusive electron [16] and for neutrino scattering on ^{12}C and ^{16}O, where good agreement with experiment and other theoretical predictions was obtained [8,17]. The combination of Hartree-Fock single-particle wave functions with the SkE2 Skyrme parametrization is especially interesting as it yields self-consistent calculations. Indeed, in such a case the same force is used for the generation of the single-particle wave functions and as residual interaction.

III. RESULTS

Figure 1 shows the dominant multipole contributions to the differential cross section for the self-consistent CRPA calculation with the SkE2 force. Most strength is supplied by transitions to negative parity $J^\pi=1^-$ and $J^\pi=2^-$ states, with considerable additional contributions of $J^\pi=1^+$ and $J^\pi=2^+$ transitions. Multipoles up to $J=6$ were included in the calculation, higher-order contributions were found to be negligible for the total cross section. The large number of peaks showing up in the plot is characteristic for a $1p$-$1h$ CRPA calculation in heavy nuclei. This behavior, however, complicates the energy integration of the results. Therefore, the calculation was done for all multipoles separately and with a dynamic grid, adding more integration points where needed, until convergence was reached. The smooth behavior of the curve in Fig. 4 assures that this integration is indeed well under control.

The calculation was repeated with different sets of single-particle parameters. Table I summarizes these results and lists the dominant multipole contributions for different approaches. These include calculations with Woods-Saxon single-particle wave functions and a Landau-Migdal residual interaction. Moreover, the influence of the exact position of the single-particle threshold was examined. Although the overall behavior of the differential cross section is to a large extent the same for the three calculations, important differences exist between the total cross sections. Whereas the total cross section is fairly independent of the used single-particle wave functions and the residual interaction, we observe a much stronger influence of the single-particle energy input used in the Hartree-Fock Skyrme CRPA calculation. The self-consistent calculation based on the Skyrme force and the Woods-Saxon Landau-Migdal calculation produce results that are identical at the level of 5%. The Skyrme

TABLE I. Comparison between different multipole contributions to the ω-integrated ^{208}Pb(ν, ν')^{208}Pb* cross section for various choices of the single-particle properties and residual interaction in the CRPA calculations. The incoming neutrino energy was 50 MeV.

	total (10^{-42} cm^2)	$J^\pi=1^+$(%)	$J^\pi=1^-$(%)	$J^\pi=2^+$(%)	$J^\pi=2^-$(%)	$J^\pi=3^+$(%)
Hartree-Fock+SkE2 (self-consistent)	499	9.0	40.5	12.3	21.8	9.4
Hartree-Fock+SkE2 ($S_n=7.37$ MeV)	645	20.6	28.7	10.9	24.2	9.0
Woods-Saxon+Landau-Migdal ($S_n=7.37$ MeV)	517	20.7	30.0	9.92	22.1	10.3

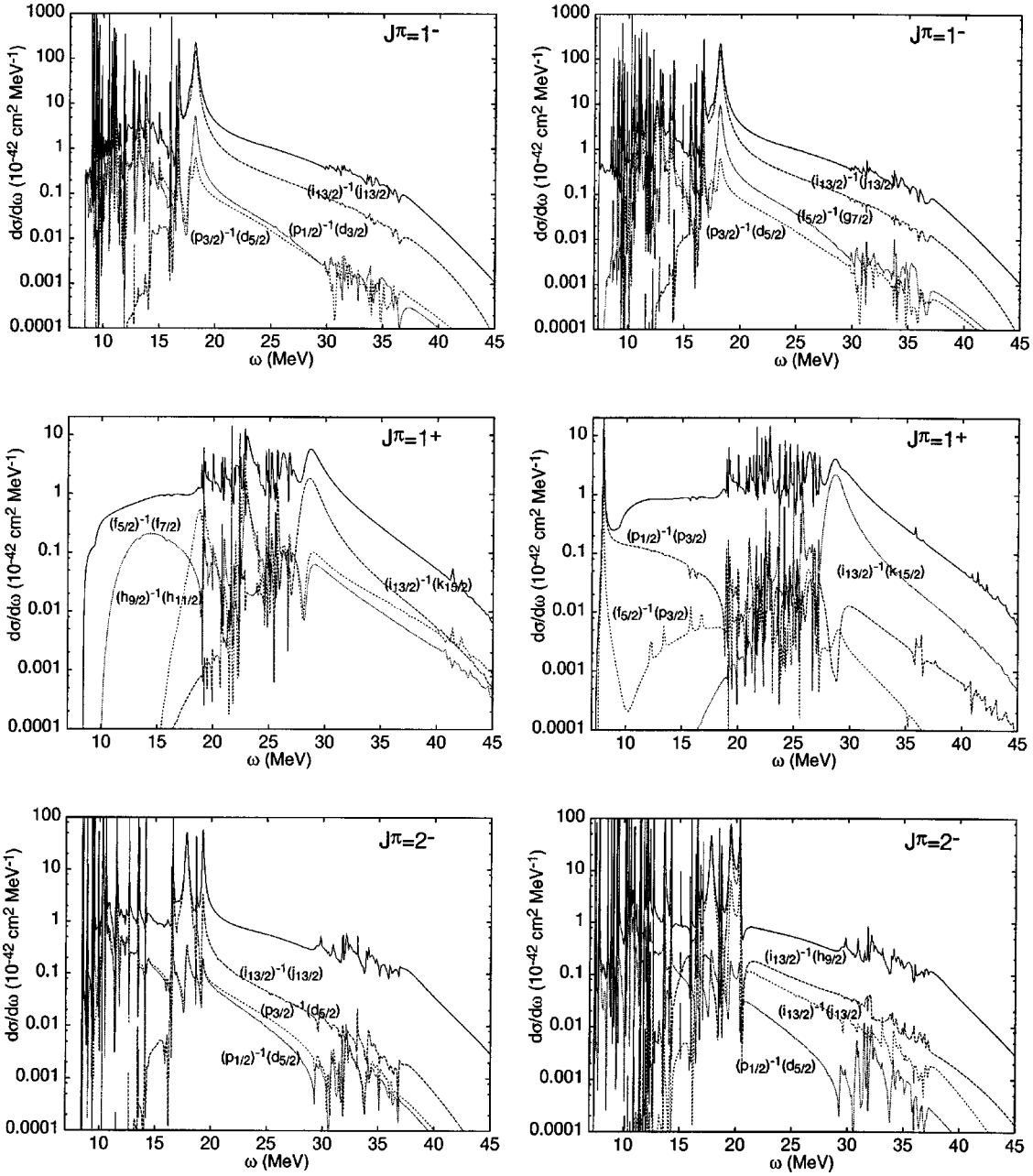

FIG. 2. Dominant neutron single-particle channels for the $J^\pi=1^-$, $J^\pi=1^+$, and $J^\pi=2^-$ transitions. The left panels show the results for the self-consistent Hartree-Fock Skyrme CRPA calculation, for the right panels the Hartree-Fock single-particle thresholds were replaced by the experimental values. The incoming neutrino energy is 50 MeV.

calculation turns out to be particularly sensitive to the choices made with regard to the single-particle energies. Slightly shifting the value of the neutron threshold from the self-consistently obtained value of 8.4 MeV to the real threshold of 7.4 MeV results in an enhancement of the cross section of about 30%. This feature can be attributed to the fact that a large fraction of the strength is residing right above the particle-emission threshold. Table I shows that relative contributions from the $J^\pi=2^-,2^+$ and $J^\pi=3^+$ multipoles are in excellent agreement. Whereas the $J^\pi=1^-$ and 2^- multipoles exhaust the largest part of the integrated strength, the dominance of $J^\pi=1^-$ is substantially more distinct in the fully self-consistent calculation. This, however, goes hand in hand with a suppression of $J^\pi=1^+$ transitions, compensating the differences in total strength with the Woods-Saxon Landau-Migdal results. For both Hartree-Fock calculations, this difference in $J^\pi=1^+$ strength, however, remains the main cause of the discrepancy in total results.

The results of a further analysis of these differences are shown in Fig. 2. The left panels give the most important single-particle channels for the dominant multipole contributions to the self-consistent CRPA calculation, the right panels contain similar results but now obtained with the adjusted single-particle energies to comply with experimental values for the neutron threshold. The $J^\pi=1^-$ and 2^+ results for both calculations are in fair agreement, with only minor dif-

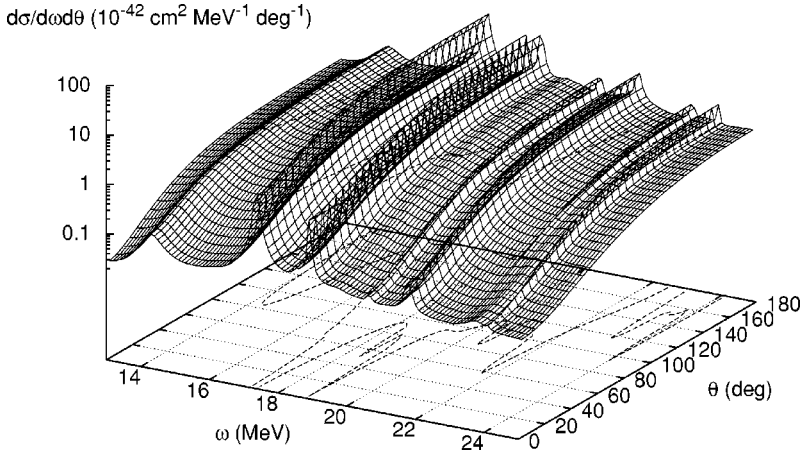

FIG. 3. Cross section for the reaction $^{208}\mathrm{Pb}(\nu,\nu')^{208}\mathrm{Pb}^*$ as a function of the excitation energy of the nucleus and the scattering direction of the lepton. The incoming neutrino energy is 50 MeV. Single-particle wave functions were obtained with a Hartree-Fock calculation, the residual interaction is the SkE2 Skyrme parametrization.

ferences between the cross sections. For $J^\pi = 1^+$ transitions an obvious discrepancy shows up in the resonance arising between 7 and 8 MeV. This difference is clearly due to the 1^+ resonance being shifted into the continuum by the adaptation of the single-particle energies. The extra strength is related to the experimentally observed giant $M1$ resonance [18], centered (7.3 MeV) almost exactly on the neutron-emission threshold and with a width of approximately 1 MeV. Experimentally, it is found that more than half of this observed $M1$ strength lies below the threshold, and therefore will not contribute to neutron emission [18]. As the difference between both calculations in Fig. 2 already suggests, the position of this resonance presents a major complication in the exact determination of the knockout of low-energy neutrons. Unlike the former work [19] where the $(i_{13/2})^{-1}(i_{11/2})$ contribution was found to be the most important channel in the 1^+ strength, we only observe this channel to be prominent in the Woods-Saxon Landau-Migdal calculation. The self-consistent calculation shows the $(i_{13/2})^{-1}(k_{15/2})$ channel as the most important neutron contribution. The shift in threshold energies favors the $(p_{1/2})^{-1}(p_{3/2})$ and $(f_{5/2})^{-1}(p_{3/2})$ neutron channels, giving rise to the 1^+ resonance between 7 and 8 MeV.

Figure 3 shows the cross section as a function of the excitation energy of the nucleus and the angular distribution of the outgoing lepton. The cross section is clearly backward peaked, a result that was also found in light nuclei for neutral-current reactions in this energy range [8].

In Fig. 4, the dependence of the total $^{208}\mathrm{Pb}(\nu,\nu')^{208}\mathrm{Pb}^*$ cross section on the incoming neutrino energy is studied. This behavior basically reflects the fact that the cross section is proportional to the square of the outgoing lepton energy. Moreover, the plot shows that neutrino cross sections are slightly larger than cross sections for the scattering of antineutrinos, a difference growing with increasing neutrino energy. A comparison with previous studies reveals that for larger incoming energies, our cross sections overshoot those of Refs. [5,7] considerably. This can probably be attributed to the more accurate description of the energy continuum provided by the CRPA formalism. At intermediate energies, our results are in good agreement with those of Ref. [5], whereas for energies below approximately 50 MeV, the cross

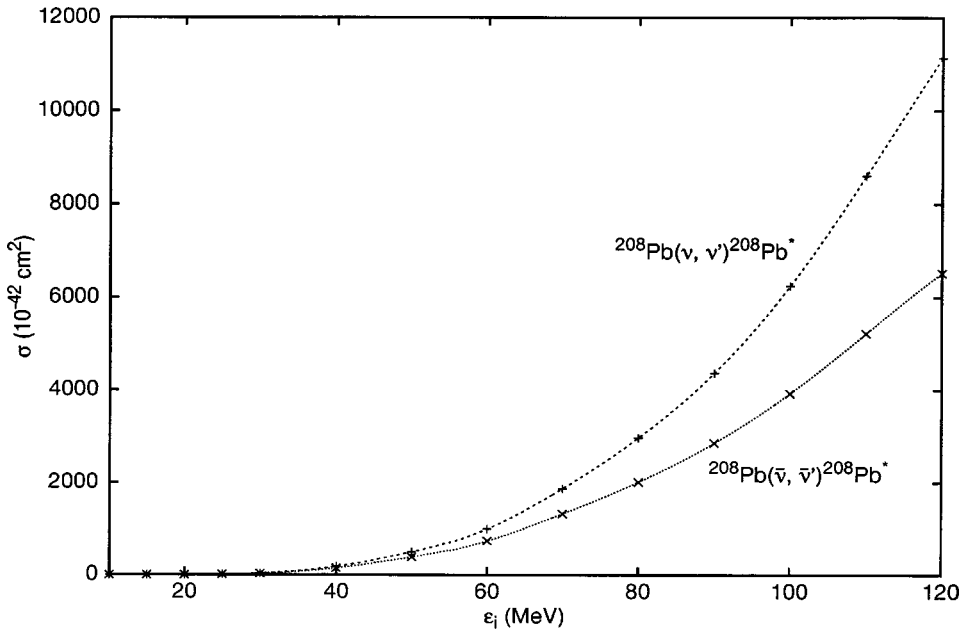

FIG. 4. $^{208}\mathrm{Pb}(\nu,\nu')^{208}\mathrm{Pb}^*$ and $^{208}\mathrm{Pb}(\bar{\nu},\bar{\nu}')^{208}\mathrm{Pb}^*$ cross sections as a function of the energy of the incoming neutrino for the self-consistent Hartree-Fock Skyrme calculation. Note that only transitions to continuum states are included in the CRPA calculation.

TABLE II. Branching ratios (in units of 10^{-42} cm^2) for the neutral-current neutrino-scattering reaction on ^{208}Pb, as obtained within the CRPA formalism.

	Hartree-Fock + SkE2	Woods-Saxon + Landau-Migdal
^{208}Pb($\nu, \nu' p$) ^{207}Tl	35	34
^{208}Pb($\nu, \nu' n$) ^{207}Pb	464	483
Total	499	517

sections obtained in the present work become smaller than those of previous studies [5,7]. Of course, this is partly due to the fact that the CRPA formalism only includes transitions to particle-unbound states, while the results given in Ref. [5] also take transitions to states below the neutron-emission threshold into account. However, a comparison of neutron branching ratios between both studies (see Table II) reveals that bound-state contributions cannot fully explain the differences [5,20]. Since the neutrino signal will be studied experimentally through the induced neutron knockout, the omission of bound-state contributions in the CRPA calculations does not affect the relevance of our results.

In order to obtain more information about supernova neutrinos, the cross section has to be folded with the appropriate energy distribution. References [21,22] advocate Fermi-Dirac spectra with temperatures around 8 to 10 MeV for heavy flavor neutrinos not taking part in charged-current reactions, and decoupling closer to the center of the supernova, 5 MeV for electron antineutrinos, and even slightly lower values for electron neutrinos interacting with the larger number of neutrons in the star core. The shape of the spectrum is most accurately described when a chemical potential is included. The energy distribution is then given by

$$n_\nu(E, T, \alpha) = \frac{N_\alpha}{T^3} \frac{E^2}{1 + e^{E/T - \alpha}}, \tag{1}$$

with T the temperature of the spectrum, α the degeneracy parameter associated with the chemical potential μ,

$$\alpha = \frac{\mu}{T}, \tag{2}$$

and N_α the normalization factor for the distribution, only depending on α. In Fig. 5 we study the evolution of the total neutral-current cross section on ^{208}Pb for a variety of neutrino-energy distributions, with the cross sections averaged over neutrino and antineutrino contributions. With increasing temperature a broadening of the spectrum emerges, and there is a shift of the neutrino energies to higher values. This explains the steep rise in the cross section when the spectrum temperature is going up. Not only the average neutrino energy is rising, but also relatively more high-energy neutrinos are contributing. The introduction of a chemical potential in a spectrum at fixed neutrino temperature increases the average neutrino energy, but meanwhile causes a suppression of the high-energy tail of the spectrum. This is clearly reflected by the plot; at fixed neutrino temperature a nonvanishing chemical potential enhances the cross section. On the other hand, the inclination of the dotted lines linking spectra with equal average neutrino energies shows that for distributions with the same average energy, spectra with a higher chemical potential result in smaller cross sections. This is easily explained by the observation that due to the depletion of the high energy part of the spectrum, less high-energy neutrinos will be arriving, reducing the response in a terrestrial detector accordingly. As observed before, our cross-section results tend to be smaller than previous studies for small values of the incoming neutrino energy. Due to the relatively small energies of the supernova neutrinos, our folded cross sections are considerably reduced compared to those of other authors. A major cause of uncertainty is the position of the $M1$ resonance at the threshold where an exact contribution of this resonance to neutron emission is delicate to establish.

IV. CONCLUSIONS

In summary, we studied neutral-current neutrino scattering on the nucleus ^{208}Pb within a CRPA formalism. Taking into account the differences between the various approaches,

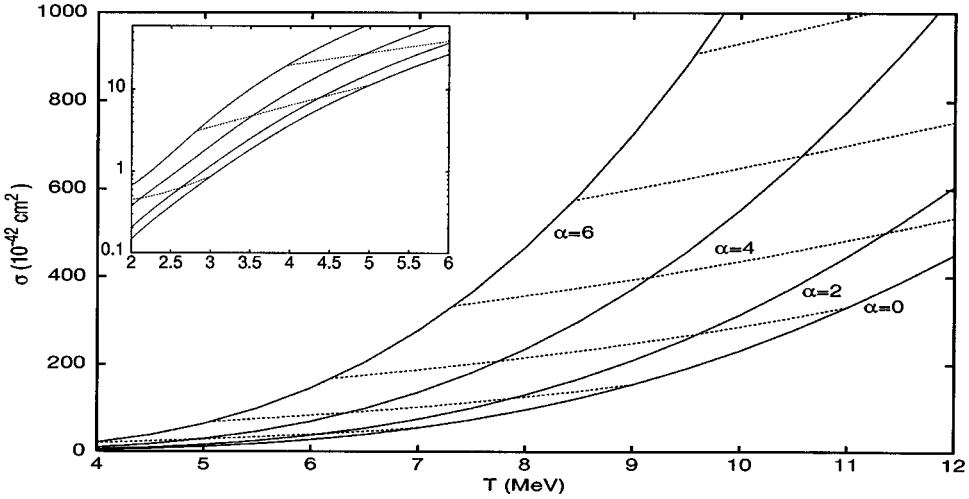

FIG. 5. Total cross section for neutral-current neutrino scattering on ^{208}Pb, averaged over neutrinos and antineutrinos, and folded with a Fermi-Dirac spectrum as a function of the temperature T and the chemical potential of the neutrino energy distribution. The dotted lines connect spectra with the same average energy. Note that the inset uses a log scale to make the behavior at small temperatures values more clear.

the cross-section results are in line with previous calculations. The major multipole contributions stem from $J^\pi = 1^-$, $J^\pi = 2^-$, and $J^\pi = 1^+$. The computed cross sections appear to be relatively model independent. Indeed, changes in the single-particle wave functions and the residual interactions do only marginally affect the final results. A major cause of uncertainty is the position of the $M1$ resonance at the threshold where an exact contribution of this resonance to neutron emission is delicate to establish, and the calculation is extremely sensitive to the input of single-particle energies.

In order to obtain information relevant for the terrestrial detection of supernova neutrinos, the cross-section results have to be folded with the energy distribution of the neutrinos. The fact that the cross sections obtained in the present work tend to be smaller than those of Refs. [5,7] at low neutrino energies, combined with the sensitivity of the spectrum to the contribution of small values of the incoming neutrino energies then implies a response that is considerably smaller than that of previous studies.

ACKNOWLEDGMENTS

The authors would like to thank E. Kolbe, G. Martínez-Pinedo, P. Vogel, and A. Murphy for interesting discussions. N.J. is grateful to the Fund for Scientific Research (FWO), Flanders, for financial support and to the physics department of the University of Basel for its hospitality.

[1] J.F. Beacom, R.N. Boyd, and A. Mezzacappa, Phys. Rev. Lett. **85**, 3568 (2000).
[2] J.F. Beacom, R.N. Boyd, and A. Mezzacappa, Phys. Rev. D **63**, 073011 (2001).
[3] R.N. Boyd and A.St.J. Murphy, Nucl. Phys. **A688**, 386c (2001).
[4] C.K. Hargrove *et al.*, Astropart. Phys. **5**, 183 (1996).
[5] E. Kolbe and K. Langanke, Phys. Rev. C **63**, 025802 (2001).
[6] C. Volpe, N. Auerbach, G. Colo, and N. Van Giai, Phys. Rev. C **65**, 044603 (2002).
[7] G. Fuller, W.C. Haxton, and G.C. McLaughlin, Phys. Rev. D **59**, 085005 (1999).
[8] N. Jachowicz, S. Rombouts, K. Heyde, and J. Ryckebusch, Phys. Rev. C **59**, 3246 (1999).
[9] G.F. Bertsch and S.F. Tsai, Phys. Rep. **18**, 125 (1975).
[10] S.F. Tsai, Phys. Rev. C **17**, 1862 (1978).
[11] G. Co' and S. Krewald, Phys. Lett. **137B**, 145 (1984).
[12] M. Waroquier, K. Heyde, and G. Wenes, Nucl. Phys. **A404**, 269 (1983).
[13] M. Waroquier, G. Wenes, and K. Heyde, Nucl. Phys. **A404**, 298 (1983).
[14] G.A. Rinker and J. Speth, Nucl. Phys. **A306**, 360 (1978).
[15] J. Ryckebusch, M. Waroquier, K. Heyde, J. Moreau, and D. Ryckbosch, Nucl. Phys. **A476**, 273 (1988).
[16] V. Van der Sluys, J. Ryckebusch, and M. Waroquier, Phys. Rev. C **51**, 2664 (1995).
[17] N. Jachowicz, K. Heyde, J. Ryckebusch, and S. Rombouts, Phys. Rev. C **65**, 025501 (2002).
[18] R.M. Laszewski, R. Alarcon, D.S. Dale, and S.D. Hoblit, Phys. Rev. Lett. **61**, 1710 (1988).
[19] D. Cha, B. Schwesinger, J. Wambach, and J. Speth, Nucl. Phys. **A430**, 321 (1984).
[20] E. Kolbe (private communication).
[21] H.-T. Janka and W. Hillebrandt, Astron. Astrophys. **78**, 373 (1998).
[22] H.-T. Janka and W. Hillebrandt, Astron. Astrophys. **224**, 49 (1998).